

COMPOSITE FAILURE ANALYSIS OF AN AIRCRAFT STRUCTURE

Ricardo Afonso Angélico, ricardoangelico@gmail.com

Marcelo Leite Ribeiro, strova@hotmail.com

Marcus Vinicius Angelo, marcus.angelo@usp.br

Volnei Tita, voltita@sc.usp.br

Escola de Engenharia de São Carlos - Universidade de São Paulo, Av. Trabalhador São-carlense, 400, Pq Arnold Schmidt, São Carlos - SP

Abstract. *The objective of the present work is to analyze the progressive failure process of an aircraft structure made of composite materials. These materials combine the properties of its constituents (fiber, resin and interface) in order to improve the performance against the use of phases alone. The combination of the phases can join characteristics such as low density and high strength, which are desired in the aerospace segment, because it can increase the autonomy or aircraft payload. The inherent anisotropy turns difficult the prediction of failure mechanisms, and consequently, the overall behavior of the structure. This work presents a phenomenological composite material model which is applied on the finite element analyses of structures under flexural loads. The material model is implemented in an UMAT subroutine, which is compiled and linked to the finite element package Abaqus[®]. Two kinds of structure are investigated. The first one consists of the 3-point bending problem for two different stacking sequences. In this study, the results of computational simulations are compared with experimental results. The material model showed to be able to predict the stiffness and strength reductions, induced by progressive failure of composite laminate. In the second, it is investigated an aircraft beam. For both cases, there are presented the global structure behavior through the force versus displacement response.*

Keywords: *aircraft structure, composite materials, progressive failure analysis*

1. INTRODUCTION

Composites are multiphase materials which have a significant part of properties from each phase, in order to obtain a material with better performance when compared to the phases alone (Callister, 2007). In general, there is a stiffer and strength phase called reinforcement or dispersed phase, and with a phase less stiffness and strength called matrix or continuum phase (Daniel and Ishai, 2006). The combination of the phases results in an anisotropic media, with higher properties aligned to the reinforcement direction. According to the structural design, the anisotropy has advantages and disadvantages. The anisotropy enables to design the structural component and the material together, since the fibers can be aligned to the direction of the major loads. Thus, it becomes possible to obtain a structure of higher performance, more strength, and stiffness and with low weight. However, the anisotropy turns difficult the prediction of failure modes, which now can be linked with the reinforcement failure, the matrix failure or the interface between both, under different types of load (tensile, compression, shear).

The mechanical behavior of composite materials has been studied by many researches, looking for developing failure criteria able to predict reasonably the failure of an anisotropic and heterogeneous media, as well as, degradation laws that decrease the material properties according to the failure verified and guaranteeing the consistency of physical processes.

The possibility of designing lighter structures is desired for several segments, in particular, for the aeronautical industry. The application of the materials with high specific properties can enable an increasing of the aircraft payload or mission range. Under this motivation, a material model composed by a failure criteria and degradation laws is applied on the study of an aircraft structure. First of all, it is show the material model and the parameters associated. Second, the material model is initially evaluated for a composite shell submitted on 3-point bending test for two different stacking sequences. It is important to mention that the computational results are compared to experimental results. After that, the material model is used to simulate a typical aircraft omega floor beam under flexural loads. Finally, the numerical results are discussed, showing the limitations and potentials of the material model applied for the structural failure analysis.

2. MATERIAL MODEL

2.1 Material model description

Initially, it is considered the local coordinate system in Fig. 1 where the direction 1 is parallel to the reinforcement direction, the direction 2 is orthogonal to the direction 1 and it is on the plane of the lamina, and direction 3 is normal to the both. On the analysis, the composite lamina is considered a transversely isotropic material, being the plane 2-3 an isotropic plane.

The constitutive law for a composite lamina under the plane stress hypothesis can be written according to the Eq. 1.

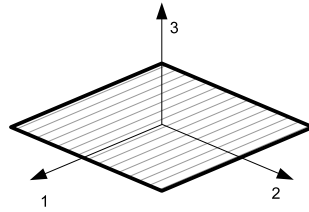


Figure 1. Local coordinate system in a transversely isotropic composite lamina

Four independent elastic material properties (E_1 , E_2 , ν_{12} and G_{12}) are necessary to write the stress-strains relations.

$$\begin{Bmatrix} \sigma_{11} \\ \sigma_{22} \\ \sigma_{12} \end{Bmatrix} = \begin{bmatrix} Q_{11} & Q_{12} & 0 \\ Q_{12} & Q_{22} & 0 \\ 0 & 0 & Q_{66} \end{bmatrix} \begin{Bmatrix} \epsilon_{11} \\ \epsilon_{22} \\ \gamma_{12} \end{Bmatrix} \quad (1)$$

$$Q_{11} = \frac{E_1}{1 - \nu_{12}\nu_{21}}; \quad Q_{22} = \frac{E_2}{1 - \nu_{12}\nu_{21}}; \quad Q_{12} = \frac{\nu_{21}E_1}{1 - \nu_{12}\nu_{21}} = \frac{\nu_{12}E_2}{1 - \nu_{12}\nu_{21}}; \quad Q_{66} = G_{12} \quad (2)$$

Where:

E_1 , E_2 : Young's modulus in longitudinal (direction-1) and transversal direction (direction-2);

G_{12} : shear modulus on the plane 1-2;

and ν_{12} : Poisson's ratio on the plane 1-2.

After the determination of the stress state in each lamina, the failure modes are verified by failure criteria. The failure criteria calculate a failure index, if this value is greater than the unit, then the material point at the lamina fails. So, it is necessary to reduce the material properties in this point at the lamina. Therefore, the material model is constituted of a failure criteria and a degradation law. In this work, there are considered five failure modes divided in two groups: fiber-failure (FF) and inter-fiber failure (IFF). In fiber-failure modes, layer can failure under longitudinal tensile loads (FF-T) and longitudinal compression loads (FF-C). The fiber-failure criteria are based on Hashin's Criteria (Hashin, 1980). The inter-fiber failure mode considers the failure on the plane normal to the longitudinal direction. In this plane are identified three failure modes: Mode A (IFF-A) (with tensile transversal stress) and Mode B (IFF-B) and Mode C (IFF-C) (with compressive transversal stress). The inter-fiber failure modes are based on Puck's Criteria (Puck and Shürmann, 1998) (Puck and Shürmann, 2002) (Puck and Shürmann, 1998). In this work, Puck failure criteria is written for 2D (Knops, 2008). The failure criteria can be written through the relations expressed in Eq. 3 until Eq. 7.

FF - T: fiber failure under tensile stress ($\sigma_{11} > 0$):

$$f_{FF} = \left(\frac{\sigma_{11}}{F_{1T}} \right)^2 + \left(\frac{\sigma_{12}}{F_{12}} \right)^2 \quad (3)$$

FF - C: fiber failure under compressive stress ($\sigma_{11} < 0$):

$$f_{FF} = \left(\frac{\sigma_{11}}{F_{1C}} \right)^2 \quad (4)$$

IFF - A: inter-fiber failure Mode A ($\sigma_{22} \geq 0$):

$$f_{IFF} = \sqrt{\left[\left(\frac{1}{R_{\perp}^t} - \frac{p_{\perp||}^t}{R_{\perp||}} \right) \cdot \sigma_{22} \right]^2} + \left(\frac{\sigma_{12}}{R_{\perp||}} \right)^2 + \frac{p_{\perp||}^t}{R_{\perp||}} \sigma_{22} \quad (5)$$

IFF - B: inter-fiber failure Mode B ($\sigma_{22} < 0$ e $|\sigma_{22}/\sigma_{12}| \leq |R_{\perp\perp}^A/\sigma_{12,c}|$):

$$f_{IFF} = \sqrt{\left(\frac{\sigma_{12}}{R_{\perp||}} \right)^2 + \left(\frac{p_{\perp||}^c}{R_{\perp||}} \sigma_{22} \right)^2} + \frac{p_{\perp||}^c}{R_{\perp||}} \sigma_{22} \quad (6)$$

IFF - C: inter-fiber failure Mode C ($\sigma_{22} < 0$ e $|\sigma_{22}/\sigma_{12}| \geq |R_{\perp\perp}^A/\sigma_{12,c}|$):

$$f_{IFF} = \left[\left(\frac{\sigma_{12}}{2(1+p_{\perp\perp}^c)R_{\perp||}} \right)^2 + \left(\frac{\sigma_{22}}{R_{\perp||}^c} \right)^2 \right] \frac{R_{\perp||}^c}{-\sigma_{22}} \quad (7)$$

Where:

$R_{||}^t$: longitudinal strength under uniaxial tensile $\sigma_{||}^t$;
 R_{\perp}^t : transverse strength under uniaxial compressive σ_{\perp}^t ;
 R_{\perp}^c : transverse strength under uniaxial compressive σ_{\perp}^c ;
 $R_{\perp||}$: longitudinal strength under shear, under pure shear action $\tau_{\perp||}$;
 $R_{\perp\perp}^A$: fracture plane strength under action of $\tau_{\perp\perp}$ in this plane;
 $p_{\perp||}^t, p_{\perp||}^c, p_{\perp\perp}^c$: slopes on failure surface.

$$R_{\perp\perp}^A = \frac{R_{\perp}^c}{2(1 + p_{\perp\perp}^c)} \quad (8)$$

$$R_{\perp||} = \frac{p_{\perp||}^c}{p_{\perp\perp}^c} R_{\perp\perp}^A \quad (9)$$

$$\tau_{12,c} = R_{\perp||} \cdot \sqrt{1 + 2p_{\perp\perp}^c} \quad (10)$$

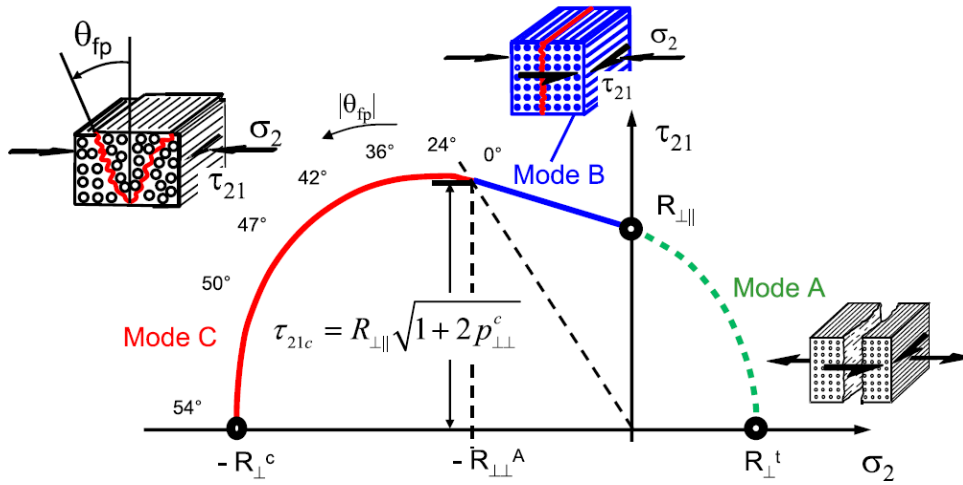


Figure 2. Inter-fiber failure envelope (Knops, 2008).

Associated with the failure modes, there are degradation laws where mechanical properties are conveniently decreased. If the lamina failures under FF-T or FF-C ($f_{FF} > 1$), the longitudinal Young's Modulus (E_1) are reduced according to the Eq. 11 (Matzenmiller, 1995), and the transverse properties (E_2 , ν_{12} and G_{12}) are reduced to zero (Tab. 1).

$$\omega = 1 - \exp \left[-\frac{1}{me} \left(\frac{\epsilon_{11}}{\epsilon_f} \right)^m \right] \quad (11)$$

Table 1. Degradation law for fiber failure modes ($f_{FF} > 1$).

Original properties	Degraded properties
E_1	$E_1 = (1 - \omega)E_1$
E_2	$E_2 = 0$
G_{12}	$G_{12} = 0$
ν_{12}	$\nu_{12} = 0$

If the lamina failures under IFF modes ($f_{FF} > 1$), the longitudinal properties are not changed, and the transverse properties (E_2 and G_{12}) are reduced according to the Eq. 12. Table 2 shows how the material properties are degraded for IFF modes.

$$\eta = \frac{1 - \eta_r}{1 + c(f_{IFF} - 1)^\xi} + \eta_r \quad (12)$$

Equation 11 parameters are determined through an axial tensile and compression tests of $[0]_n$ specimens, following orientations of ASTM standards tests, developed during Tita's PhD work (Tita, 2003). Typical values for parameters of

Table 2. Degradation law for inter-fiber failure modes ($f_{IFF} > 1$).

Original properties	Degraded properties
E_1	$\bar{E}_1 = E_1$
E_2	$\bar{E}_2 = \eta_E E_2$
G_{12}	$\bar{G}_{12} = \eta_G G_{12}$
ν_{12}	$\bar{\nu}_{12} = \nu_{12}$

Eq. 12 are recommended by Puck and Shürmann (1996, 2002) and Knops (2008) for carbon-epoxy composites. Table 3 shows the material elastic properties and strength values applied on finite element models.

The constitutive relations (Eq. 1), the failure criteria and the degradation laws, were implemented using the *User-Material* subroutine (UMAT) written in Fortran and linked to the finite element package Abaqus in order to be used in the Finite Element Analysis (FEA). The preliminary evaluation of the material model was performed using the 3-point bending problem, and the numerical results obtained are compared to experimental tests (Tita, 2003).

Table 3. Mechanical properties of unidirectional composite lamina (prepreg M10 - Hexcel) with a fiber volume of 63%.

Elastic properties	
Young's modulus (GPa)	$E_1 = 100; E_2 = E_3 = 10$
Shear modulus (GPa)	$G_{12} = G_{13} = 5.4; G_{23} = 3.05$
Poisson's ratio	$\nu_{12} = \nu_{13} = 0.34; \nu_{23} = 0.306$
Strength values	
Tensile strength (MPa)	$F_{1T} = 1400; F_{2T} = F_{3T} = 47$
Compression strength (MPa)	$F_{1C} = 700; F_{2C} = F_{3C} = 130$
Shear strength (MPa)	$F_{12} = F_{13} = 53; F_{23} = 89$

2.2 Preliminary material model evaluation

The FEA consists on a shell structure simply supported under the action of a loading applicator on the middle span, i.e. a typical 3-point bending test. The structure has 80 mm of length, 25 mm of width and a span of 58 mm between supports. The interface among the structure and the supports are modeled using Hard Contact (Abaqus, 2007). The supports have a diameter of 8 mm and are considered rigid. The finite element mesh is generated using S4 elements, which are a fourth-node shell elements with full integration (2 x 2), and three integration points through the thickness for each layer, totalizing $12n$ integration points by element (where n is the total number of layers). Figure 2 shows the finite element model. Small time step sizes were used at the beginning of the nonlinear analysis in order to guarantee the contact convergence. The initial time step adopted for the analyses is 1% of the total displacement applied (8 mm). Therefore, the FEA was controlled by displacement prescribed at the reference point in the loading applicator.

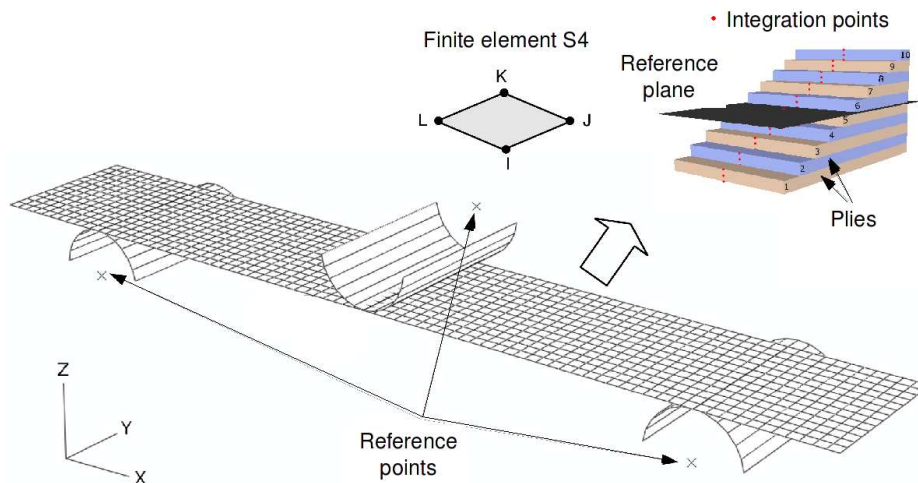


Figure 3. 3-point bending finite element model.

The 3-point bending problem is investigated for two laminates with different stacking sequences as shown in Tab. 4. The plies of Laminate 1 have 0.173 mm and of Laminate 2 have 0.177 mm of thickness.

Table 4. Laminates stacking sequences and total thickness.

	Stacking sequences	Total thickness
Laminate 1	$[0^\circ]_{10}$	1.73 mm
Laminate 2	$[0^\circ/90^\circ/0^\circ/90^\circ/0^\circ]_5$	1.77 mm

For Laminate 1 (Fig. 4(a)), in the Region I (between 0 and 4 mm of displacement), the numerical results follow the experimental average. In the Region II, the model captures the abrupt fall of force level, but it is not remain inside the experimental envelope. The equilibrium is restored for a force of 600 N for both (experimental and computational). The analysis proceeds until 5.2 mm of displacement, when stopped because of convergence problems.

For Laminate 2 (Fig. 4(b)), in the Region I, the model is representative of global structure behavior following the experimental results average. In the Region II, the model predicts the force and stiffness reduction for displacements between 5.1 and 6.5 mm, inside the experimental envelope. For displacements large than approximately 7 mm the force vs. displacement response returns to the inside of experimental envelope.

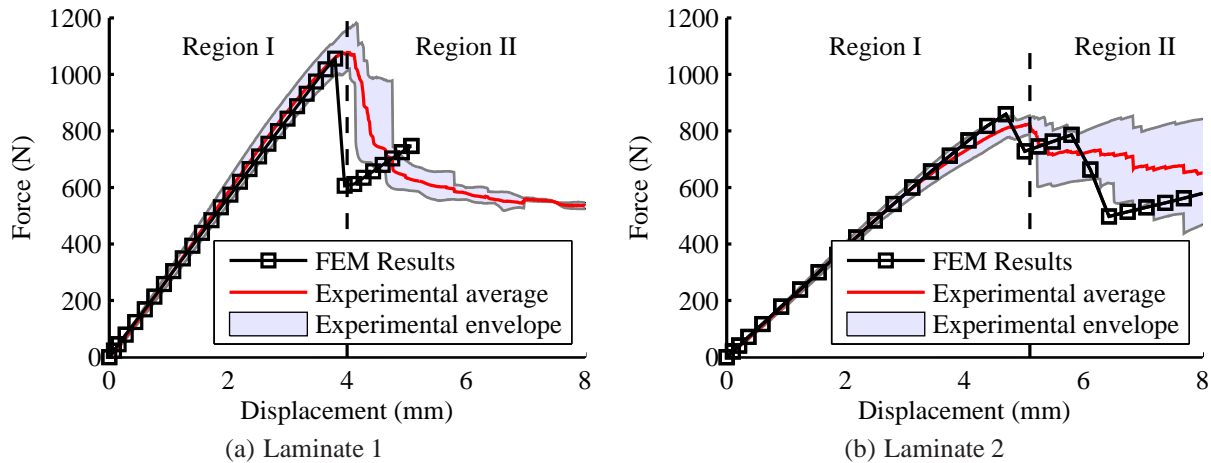


Figure 4. Comparison of computational simulations with experimental results

The errors associated to the prediction of displacement and force magnitude are shown in Tab. 5 compared to the experimental verification using the experimental results. The force vs. displacement graphs (Fig. 4) show that the material model is able to predict reasonably the force and displacement magnitude of abrupt fall, as well as, the material model estimates the progressive failure process of the laminate.

Table 5. 3-point bending results.

Laminate	Displacement (mm)			Force (N)		
	FEM	Exp.	Error	FEM	Exp.	Error
Laminate 1	3.8	4.0	5.0%	1056	1100	4.0 %
Laminate 2	4.4	5.1	13.7%	815.0	825.0	1.2 %

3. CASE STUDY

The proposed material model was evaluated using 3-point bending tests, identifying the losses of stiffness and total reaction force. This material is now applied on the study of a more complex structure, a generic composite aircraft floor-beam under flexural loads. In general, the critical cases of these flexural loads is due to transferred efforts of passenger accents under emergency landing where high loads factors are considered and required by the aeronautical authorities. Thus, the objective is to investigate the global structure behavior, through the force vs. displacement response, considering a progressive failure analysis. For this, a finite element model of a omega floor beam was developed and linked to the user subroutine of the material model.

Figure 3 shows the finite element model. The beam ends are fixed (all DOFs are restricted) and in the middle span is applied a uniform distributed pressure. The analysis is progressive and the equilibrium is each time step is verified for the

actual configuration (geometric nonlinearity). The same finite element of the previous analysis is used (Element S4). A refined mesh was necessary to ensure a smooth transfer of loads from the top of the beam to the walls.

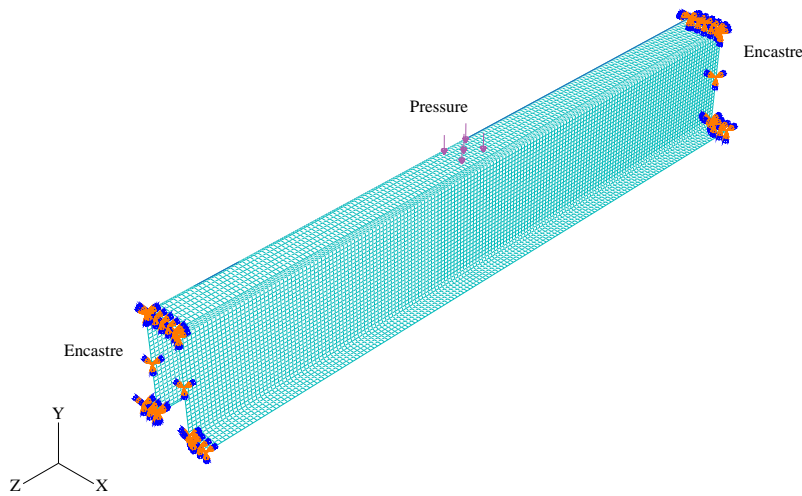


Figure 5. Floor-beam finite element model.

Figure 3 shows the global force vs. displacement response, where the marks on the curves indicates the time steps of the nonlinear analysis that satisfies equilibrium. The force is calculated through the sum of y-components of reaction forces at beam ends, and it is considered the displacement at the center of region where the pressure is applied. For a displacement of 1.8 mm, the reduction of curve slope indicates a stiffness structural loss. After a displacement of 1.8 mm, the analysis converges for a displacement of 2.7 mm. Thus, the global structure stiffness needs to be considered for displacements larger than 2.7.

Between 1.4 mm and 1.8 mm, it can be seen that the material model curve departs from the linear material curve, indicating that the processes of failures starts before the abrupt structural stiffness change in 1.8 mm. At this displacement level, the failure occurs in several layers simultaneously, that justifies the significant change in the curve.

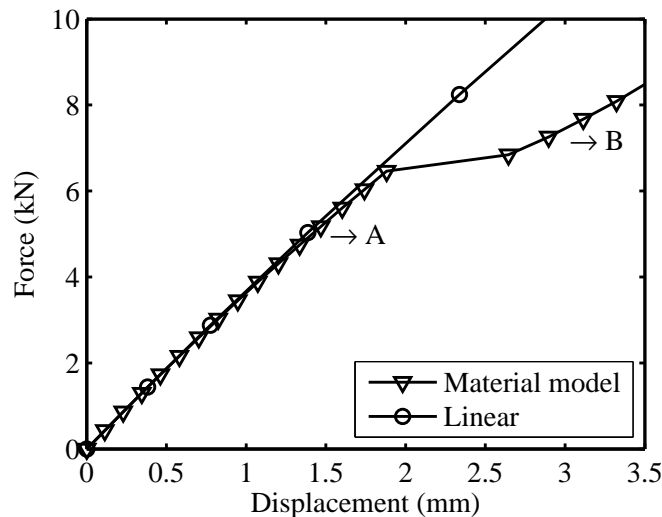


Figure 6. Floor-beam finite element model.

In order to illustrate the stress distributions before and after the stiffness change, Fig. 7 shows the σ_{11} component for the levels of displacement A (1.6 mm, 5 kN) and B (3.1 mm, 7 kN). The curvature of the beam between the top and the walls confers a stiffening to the structure, so the distribution of efforts is concentrated in the region where the pressure load is applied. Only with a reduction of the material properties, due to the plies failures, the loads are transferred significantly to the beam walls.

The reduction of the material properties is illustrated in Fig. 8 for a level of displacement B (3.1 mm, 7 kN). Young's modulus is reduced, especially for the finite elements located more to the center of structure.

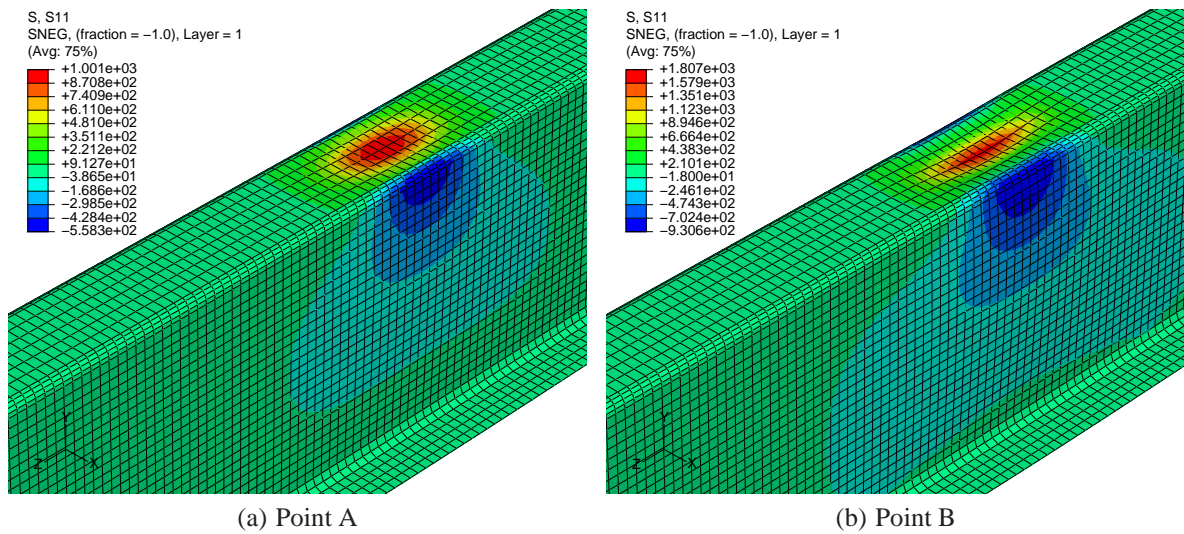


Figure 7. Stress component σ_{11} .

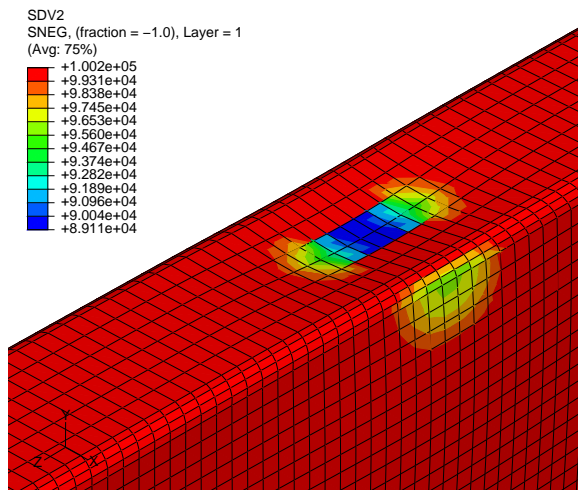


Figure 8. Longitudinal Young's modulus (E_1).

4. CONCLUSIONS

In this work, a progressive composites failure model was presented and compared with experimental results for two stacking sequences ($[0^\circ]_{10}$ and $[0^\circ/90^\circ/0^\circ/90^\circ/0^\circ]_S$) under flexural loading. From the force vs. displacement responses, it can be seen that the material model is able to represent the loss of stiffness and magnitude of force associated with the failure mechanisms.

Since the model has been evaluated, it was applied on a case study of a generic aircraft composite floor beam under flexural loads. The global structure behavior was investigated through the force vs. displacement, which shows a significant reduction of stiffness in 1.8 mm, as well as, a considerable reduction of the material properties on the region where the loads are applied.

A progressive failure analysis provides information of the global structure behavior under a failure condition. Such information may be used to estimate the loads on the component parts of the neighborhood where the fail occurred, and also, a better understanding of how the final configuration of the failed structure may affect the aircraft safety.

5. ACKNOWLEDGEMENTS

The authors would like to thank FAPESP and CNPq.

6. REFERENCES

- Abaqus Inc., 2007, Abaqus Version 6.7 Documentation, United States of America.
- Callister, W. D., 2007, "Material science and engineering: an introduction", John Wiley and Sons, Inc, 7th
- Daniel, I. M. and Ishai, O., 2006, "Engineering mechanics of composite materials", Oxford University Press, New York, 2nd
- Hashin, Z., 1980, "Failure criteria for unidirectional fiber composites", Journal of Applied Mechanics, Vol. 47, pp. 329-334
- Knops, M., 2008, "Analysis of failure in fiber polymer laminates: the theory of Alfred Puck", Springer, New York
- Matzenmiller, A., Lubliner, J. and Taylor, R. L., 1995, "A constitutive model for anisotropic damage in fiber-composites", Mechanics of materials, Vol. 20, pp. 125-152
- Puck, A. and Shürmann, H., 1996, "Failure Analysis of FRP laminates by means of physically based phenomenological models", Composite Science and Technology, Vol. 58, pp. 1045-1067
- Puck, A. and Shürmann, H., 2002, "Failure Analysis of FRP laminates by means of physically based phenomenological models", Composite Science and Technology, Vol. 62, pp. 1633-1662
- Tita, V., 2003, "Contribuição ao estudo de danos e falhas progressivas em estruturas de material compósito polimérico", Escola de Engenharia de So Carlos, Universidade de So Paulo.

7. Responsibility notice

The author(s) is (are) the only responsible for the printed material included in this paper